Comput Mech
DOI 10.1007/s00466-016-1346-3

REVIEW PAPER

Modular-based multiscale modeling on viscoelasticity of polymer nanocomposites

Ying Li[1] · Zeliang Liu[2] · Zheng Jia[3] · Wing Kam Liu[3] · Saad M. Aldousari[4] · Hassan S. Hedia[4] · Saeed A. Asiri[4]

Received: 21 April 2016 / Accepted: 12 October 2016

Abstract Polymer nanocomposites have been envisioned as advanced materials for improving the mechanical performance of neat polymers used in aerospace, petrochemical, environment and energy industries. With the filler size approaching the nanoscale, composite materials tend to demonstrate remarkable thermomechanical properties, even with addition of a small amount of fillers. These observations confront the classical composite theories and are usually attributed to the high surface-area-to-volume-ratio of the fillers, which can introduce strong nanoscale interfacial effect and relevant long-range perturbation on polymer chain dynamics. Despite decades of research aimed at understanding interfacial effect and improving the mechanical performance of composite materials, it is not currently possible to accurately predict the mechanical properties of polymer nanocomposites directly from their molecular constituents. To overcome this challenge, different theoretical, experimental and computational schemes will be used to uncover the key physical mechanisms at the relevant spatial and temporal scales for predicting and tuning constitutive behaviors *in silico*, thereby establishing a bottom-up virtual design principle to achieve unprecedented mechanical performance of nanocomposites. A modular-based multiscale modeling approach for viscoelasticity of polymer nanocomposites has been proposed and discussed in this study, including four modules: (A) neat polymer toolbox; (B) interphase toolbox; (C) microstructural toolbox and (D) homogenization toolbox. Integrating these modules together, macroscopic viscoelasticity of polymer nanocomposites could be directly predicted from their molecular constituents. This will maximize the computational ability to design novel polymer composites with advanced performance. More importantly, elucidating the viscoelasticity of polymer nanocomposites through fundamental studies is a critical step to generate an integrated computational material engineering principle for discovering and manufacturing new composites with transformative impact on aerospace, automobile, petrochemical industries.

Keywords Polymer nanocomposites · Multiscale modeling · Viscoelasticity · Material design · Finite element analysis · Molecular dynamics

✉ Ying Li
yingli@engr.uconn.edu

Zeliang Liu
zeliangliu2017@u.northwestern.edu

Zheng Jia
zheng.jia@northwestern.edu

Wing Kam Liu
w-liu@northwestern.edu

[1] Department of Mechanical Engineering & Institute of Materials Science, University of Connecticut, Storrs, CT 06269, USA

[2] Theoretical and Applied Mechanics, Northwestern University, Evanston, IL 60208, USA

[3] Department of Mechanical Engineering, Northwestern University, Evanston, IL 60208, USA

[4] Department of Mechanical Engineering, King Abdulaziz University, Jeddah 21589, Saudi Arabia

1 Introduction and motivation

Polymer nanocomposites (PNCs) have been envisioned as advanced materials for improving the mechanical performance of neat polymers used in aerospace, petrochemical, environment and energy industries [1]. With the filler size

Published online: 28 October 2016

approaching the nanoscale, composite materials tend to demonstrate remarkable thermomechanical properties, even with addition of a small amount of fillers [2,3]. These observations confront the classical composite theories and are usually attributed to the high surface-area-to-volume-ratio of the fillers, which can introduce strong interfacial effect and relevant long-range perturbation on polymer chain dynamics [1,4–8]. As such, the Young's modulus, viscoelasticity, yield stress, fracture toughness and glass transition temperature (T_g) of these materials have been dramatically changed. Despite decades of research aimed at understanding the interfacial effect and improving the mechanical performance of composite materials, it is not currently possible to accurately predict the mechanical behaviors of PNCs directly from their molecular constituents. Therefore, design of PNCs traditionally relies on the slow and in-efficient 'Edisonian' approaches.

Viscoelasticity characterizes the most important mechanical behaviors of PNCs, represented by the storage (elastic) modulus G' and loss (viscous) modulus G''. Their ratio G''/G', so-called $\tan(\delta)$, denotes the energy dissipation during the deformation process. We have $\tan(\delta) = 0$ for a metallic spring, indicating that it loses very little energy when it is stretched and let go. However, other materials, like carbon-black filled rubber, or silica filled rubber, will have larger value of $\tan(\delta)$ due to the molecular filler-rubber interface/interphase motion. In the tire manufacturing and related industry, $\tan(\delta)$ is used as the gold standard in design and evaluation the performance of tire materials [9]. In the temperature range of 40–80 °C, the rolling resistance of tire correlates directly with $\tan(\delta)$: the smaller $\tan(\delta)$, the lower rolling resistance. A higher $\tan(\delta)$ at lower temperature will lead to good wet grip. It has been recognized that 10 % of fuel used in the average car is taken for overcoming the rolling resistance of tires. By itself, the automobile rolling resistance is responsible for the astonishing 4 % of worldwide carbon dioxide emissions from fossil fuels [10]. Thus, it is another way to improve the fuel economy by lowering the rolling resistance (or $\tan(\delta)$). However, in the tire world, designers are constrained tradeoffs in which an improvement to rolling resistance has to sacrifice the wet-road grip and/or tread-wear of tire.

As shown in Fig. 1a, the value of $\tan(\delta)$ for rubber compounds has to be enlarged and reduced simultaneously at high (40–80 °C) and low (−40 to 20 °C) temperature ranges, respectively, to reduce the rolling resistance and enhance ice and wet grips. However, for the typical synthetic rubbers filled by carbon blacks, experimental results reveal that $\tan(\delta)$ value will be enlarged and reduced at high and low temperature ranges, respectively, by increasing the loading of carbon blacks (cf. Fig. 1b). Therefore, reducing $\tan(\delta)$ at 40–80 °C, however, also reduces the $\tan(\delta)$ at −40 to 20 °C. This is why the wet-grip and rolling resistance of tires are hard to

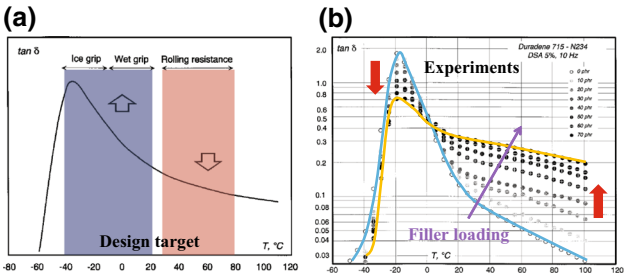

Fig. 1 **a** Design target of $\tan(\delta)$ in tire industry and **b** filler loading effect on $\tan(\delta)$ in synthetic rubber-carbon black composites observed in experiments. Note that $T_g = -67\,^{\circ}\mathrm{C}$ for rubber materials. These figures are adapted and modified from [9]

pull apart. Thus, the manufactured rubber compound cannot satisfy the requirements of tire design for targeted performance. The Transportation Research Board estimates that if tire rolling resistance were reduced by 50 %, 10 billion gallons of fuel (7.7 % of our total national fuel expenditure) could be saved per year [11]. However, it is currently unknown whether it is possible to design and manufacture the polymer compounds meeting the above requirements. Moreover, the physical mechanisms underpinning the $\tan(\delta)$ change induced by the added fillers are still not clear. These limitations and challenges call for a deeper understanding on the viscoelastic properties of PNCs and a useful toolbox for predicting these properties from their molecular constituents.

Constitutive modeling on linear elastic behaviors of PNCs dates back to the advent of micromechanics, initiated by Einstein's [12] and Smallwood's [13] two-phase model. In this model, the fillers are assumed to be spherical and rigid, immersed in an elastic polymer matrix, ignoring the aspect ratio, finite stiffness, and local changes of polymer behaviors near the fillers (interphase). Subsequent micromechanics theories have been developed through phenomenological or mean-field theoretical approaches [14–16], by using additional terms to represent these factors. Based on the finite Eshelby tensor of representative volume element [17,18], Li and co-workers have developed micromechanics models to analyze the interphase effects on effective material properties of PNCs [19], which are in good agreement with molecular dynamics simulations. Later on, these theories have been generalized to linear viscoelasticity by using the Fourier transform of the constitutive law, and some of them have explicitly considered the interphase regions in PNCs [20–23]. Besides, based on these micromechanics models, nonlinear, time-dependent constitutive models have been developed for filled elastomers, such as the Bergström-Boyce model [24–26], for finite deformation regime. These theories are relatively easy to use and fast to compute, and the sufficiently advanced ones have good descriptive capabilities and can be calibrated for multiple materials, which makes them useful for modeling and design of devices and components.

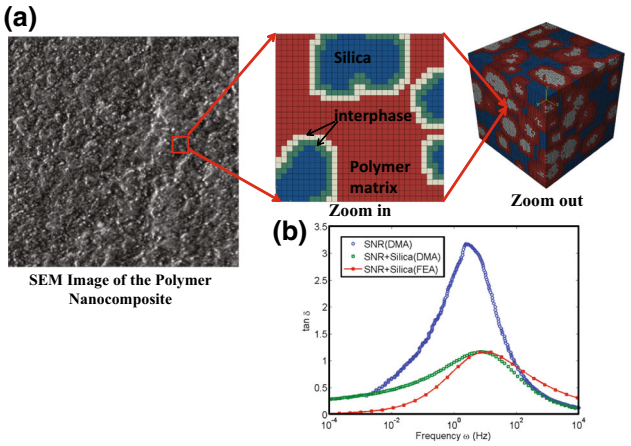

Fig. 2 **a** Finite element modeling scheme on viscoelasticity of PNCs. **b** Comparison between experimental measurements and simulation results

However, they account for interphase properties in only an approximate way. In some models, the filler is assumed to have no effect on local stress relaxation in the matrix, and in other cases, the effect is prescribed to match particular experimental observations through a fitting procedure. The common shortcoming of all existing methods is that they are based on top-down experimental data that can only be correlated with nanoscale interfacial phenomena in an indirect, case specific fashion. As such, a predictive modeling capability that is necessary for computational materials design remains to be established.

The limitations of these models and the increase in available computing power have led us to re-examine the reductionist approach. Motivated by the image-based approach pioneered by the ONR/DARPA-sponsored Dynamic 3-Dimensional Digital Structures ("D3D") project [27–29], one of the most sophisticated methods for modeling PNCs has been developed by Northwestern University in collaboration with Goodyear Tire and Rubber Company (GT), led by the corresponding author of this work, Liu, and Brinson, Chen, Dikin (among others) [30,31]. First, images of the composite microstructure obtained using scanning electron microscopy (SEM) were binarized and converted into finite element models, and interphase regions were explicitly placed around each filler particle or cluster, as shown for 2D in Fig. 2a. Reconstructed images created to reproduce the observed filler size, shape, and dispersion statistics were also considered. Afterwards, the 3D representative volume element has been reconstructed through the statistical analysis [32–34], by accurately reflecting the microstructure information revealed through SEM. Next, the constitutive behavior of the polymer matrix was determined empirically by fitting a standard phenomenological form (Prony series) to experimental results from dynamic mechanical analysis (DMA) of unfilled synthetic natural rubber. Finally, the interphase thickness and deviation from matrix constitutive behavior were then calibrated to best fit DMA results of the composite material, as shown in Fig. 2b. The difficulty arises from the thickness and properties of interphase region, which is still a debating issue [6,35–40]. Therefore, the mechanical behaviors of the interphase regime can only be calibrated from the matrix behavior for fitting the experimental data of PNCs, with predefined interphase thickness [30,41]. The result modeling scheme is a powerful methodology with sophisticated descriptive capabilities for microstructure of PNCs. However, it still suffers from the lack of predictive capability, as the interphase properties and thickness are needed to be calibrated for matching experimental data. Nevertheless, the estimated viscoelastic properties ($\tan(\delta)$) of PNCs are still far away from the experimental results in certain regime, as shown in Fig. 2b.

Essentially, all the above modeling methods are based on the micromechanics modeling strategies [30,42–45], which require the mechanical properties of different phases known as a prior. Thus, these methods are not particularly suitable for the design of PNCs, as the interphase regimes around the surface of nanoparticles are still not clear [6,46]. There is an urgent need to develop a predictive multiscale modeling scheme for PNCs, by overcoming the above limitations.

To address the above issue and challenge, the goal of our research here is to create a multiscale modeling approach that can provide guidance towards the design of materials, which necessitates predictive models of the effects of confinement and the strength of polymer-filler interaction on the resultant macroscopic behavior of PNCs. Such an effort will create a new and efficient design paradigm for the advanced PNCs. To purse this goal, a modular-based approach has been presented and discussed in this study, including four modules: (A) neat polymer toolbox; (B) interphase toolbox; (C) microstructural toolbox and (D) homogenization toolbox. Integrating these modules together, macroscopic viscoelasticity of polymer nanocomposites could be directly predicted from their molecular constituents. Through the multiscale modeling method outlined by this study, we anticipate that the design process for PNCs will be dramatically accelerated. The flexibility of the method allows for rapid computational prototyping and predicting the performance of PNCs in silico, providing new physical insights into the interplay between the molecular scale nanoparticle-polymer chain interaction and macroscopic behaviors of PNCs. Moreover, predicting the mechanical properties of PNCs a priori is the Holy Grail of material science and engineering, which is also the goal of the Grand Challenge posted by Materials Genome Initiative [47]. The modular-based multiscale modeling method could be used to obtain new paradigms for guiding experimental design of novel PNCs with large and small $\tan(\delta)$ values at low and high temperatures, respectively, satisfying

the requirements of tire materials (cf. Fig. 1a) and reducing the daily energy cost of the automobiles.

This work is organized as follow. Section 2 provides an integrated multiscale modeling scheme for understanding mechanical behaviors of PNCs. Such a multiscale modeling toolbox is based on multiple modules, which enables the flexibility of the proposed scheme. Section 3 presents a design toolbox for the viscoelasticity of neat polymer. The interphase toolbox in Sect. 4 demonstrate an efficient way to understand the chain dynamics in vicinity of nanoparticles and predict interphase properties. The microstructure information about the PNCs is given in Sect. 5. Section 6 demonstrates a self-consistent clustering analysis to homogenize the effective mechanical properties of PNCs. The perspective about design of multifunctional PNCs through multiscale modeling is discussed in Sect. 7.

2 A predictive integrated multiscale modeling scheme

A predictive integrated multiscale modeling scheme for mechanical properties of PNCs is depicted in Fig. 3, which is based on four modules:

- Module A: neat polymer toolbox. In this module, a coarse-grained molecular model, derived from systematic coarse-graining method from all-atomic simulations [48–50], has been developed. Such a model enables us to directly probe the dynamics and entanglement network of high entangled chains in molecular scale. All these observations provide the key information about the polymer dynamics and physics, which are the materials law parameters in physics-based constitutive model for finite viscoelasticity of polymers [49,51]. Therefore, parametric materials design concepts can be easily gleaned from the model. This toolbox provides the material properties of polymer matrix for direct numerical simulations (DNS) on PNCs.
- Module B: interphase toolbox. In this module, large scale molecular simulations have been performed to understand the chain dynamics in vicinity of nanoparticles [4–6], corroborated by corresponding experimental studies [52,53]. The interphase thickness and its properties will be revealed, contributing important properties in DNS modeling on PNCs.
- Module C: microstructure toolbox. The microstructure information, including dispersion of nanoparticles, their cluster size and arrangement in the space, is reconstructed through the image-based modeling scheme. The 3D representative volume element has been reconstructed through the statistical analysis [32–34], by accurately reflecting the microstructure information revealed through SEM. This toolbox yields structure information for PNCs in DNS modeling.
- Module D: PNC homogenization toolbox. According to above mechanical properties of polymer matrix and interphase, equipped with structural information, the effective mechanical properties of PNCs can be homogenized through self-consistent clustering analysis [43,54]. Therefore, the homogenized constitutive laws for PNCs could be obtained, for predicting the stress–strain curves of PNCs, their viscoelasticity and many others.

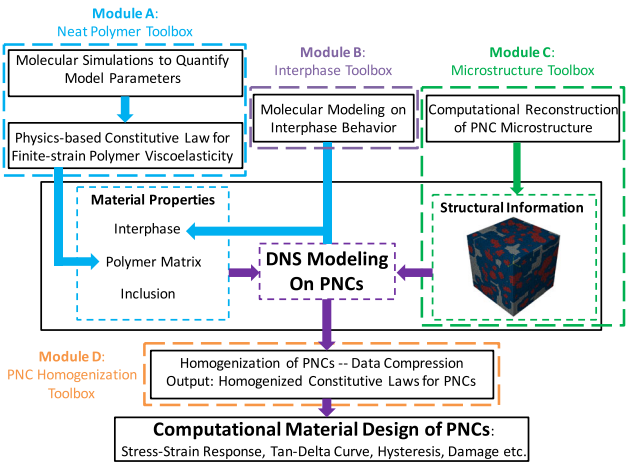

Fig. 3 An integrated multiscale modeling scheme to model and predict the mechanical behavior of PNCs by considering material properties and structural information at various length scales. The scheme consists of four modules/toolboxes: the neat polymer toolbox, the interphase toolbox, the microstructure toolbox and the PNC homogenization toolbox

Integrating above four modules together, a multiscale modeling scheme has been constructed to predict the mechanical behaviors of PNCs, by linking their various length scales. The details about these modules will be discussed and explained in the following sections. Such a modular-based systematic approach also enables the flexibility of the proposed approach.

3 Module A: neat polymer toolbox

3.1 Mechanical behaviors of polymer matrix

The prediction of mechanical behaviors of polymeric materials has been an active research area for decades. There have been numerous experimental studies addressing different aspects of the response of elastomers. Experimental evidences have accumulated that polymeric materials exhibit strong rate effects when subjected to dynamic loadings [55], showing a viscoelastic mechanical behavior. It is also well known that the stress in a polymeric specimen relaxes

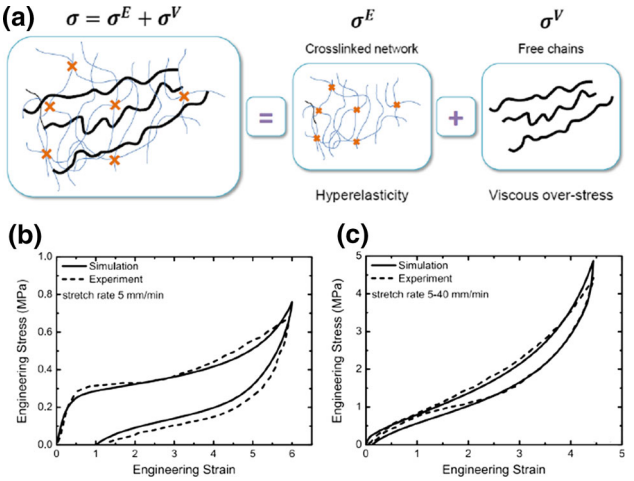

Fig. 4 **a** Microscopic structure of an elastomer can be decomposed into a cross-linked polymer network with free chains. The hyperelastic stress σ^E and viscous stress σ^V are due to the nonlinear deformation of the cross-linked network and diffusion of free chains, respectively. Therefore, the mechanical response of the elastomer can be given as $\sigma = \sigma^E + \sigma^V$. **b** Uniaxial loading and unloading behaviors of unvulcanized NR at room temperature. **c** Uniaxial loading and unloading behaviors of peroxide vulcanized NR at room temperature

towards an equilibrium state after being subjected to a fixed applied strain [56], which indicates the existence of a hyperelastic strain energy function for very low loading rates. Successful applications of polymeric materials in industry require precise prediction of the complicated mechanical behavior of polymers and thus necessitate the development of accurate constitutive equations.

The macroscopic mechanical response of elastomers originates from their microscopic molecular structure: long randomly oriented polymer chains are joined together via cross-linkers, forming a cross-linked polymeric network; free chains are randomly distributed within the cross-linked network, as illustrated in Fig. 4a. Upon loading/unloading, the cross-linked polymeric network is stretched and the free chains diffuse within the network. The cross-linked polymeric network acts as the backbone and is usually capable of recovering its original shapes after unloading, which results in a nonlinear hyperelastic mechanical response. In contrast, reptation of free chains within the cross-linked network is irreversible and causes energy dissipation (i.e. the mechanical response exhibits hysteresis upon cyclic loading), leading to a viscous mechanical behavior. Therefore, to develop a constitutive law that accurately describes the mechanical response of elastomers, their stress response needs to be decomposed into two parts [49,51,57]: a hyperelastic part and a viscous part. Physically, the hyperelastic part is attributed to the nonlinear deformation of the cross-linked polymer network, while the viscous part originates from the diffusion of the free chains.

3.1.1 Hyperelasticity of polymers

The nonlinear elasticity of a cross-linked polymeric network is typically characterized by a hyperelastic constitutive model, which is governed by a strain energy density function W. Depending on the approach followed by the authors to develop the strain energy function W, the hyperelastic models can be classified into phenomenological and physics-based models. The phenomenological models are mainly obtained from invariant-based continuum mechanics treatment of W and can be used to fit experimentally observed mechanical behaviors. The strain energy density W must depend on stretch via one or more of the three invariants of the Cauchy-Green deformation tensor. Model parameters in phenomenological models usually carry no explicit physical meaning and can only be calibrated by fitting experimental data. Physics-based models are derived based on polymer physics and statistical mechanics which begins by assuming a structure of randomly-oriented long molecular chains. The strain energy density function W for physics-based models depends on the microscopic structure of the polymeric network, in which model parameters are related to the underlying polymer physics/chemistry/dynamics and can be calibrated by using information of the microscopic structure of elastomers. Along this line, the most widely used phenomenological models include but are not limited to the Mooney Model [58], the Mooney-Rivlin Model [59], the Ogden Model [60], the Yeoh Model [61] and the Gent Model [62]. An excellent review of the detailed mathematical formulation of aforementioned phenomenological hyperelastic models is given by Marckmann and Verron [63]. For the physics-based models, there are the Neo-Hookean Model [64], the 3-Chain Model [65], the Arruda-Boyce (8-Chain) model [66], the slip-link model [67], the extended tube model [68], the non-affine micro-sphere model [69], and the non-affine network model [70]. Details about these physics-based models have been summarized and compared by Davidson and Goulbourne [70]. The Neo-Hookean Model, the 3-Chain Model and the Arruda-Boyce Model are widely deployed to characterize the hyperelastic response of elastomers because of the compact mathematical form. However, these models cannot capture the stress softening behavior observed in elastomers with low cross-linking density since they ignore the effect of polymer entanglements [70]. The extended tube model and the non-affine microsphere model can capture the stress softening but contains some parameters without clear physical connections or hard to be calculated [70]. Slip-link model and the non-affine network model can capture the stress softening and all their material parameters are connected to molecular quantities. It is worth noting that the non-affine network model is mathematically compact compared to the slip-link model, which facilitates its application in capturing stress-stretch response of elastomers [51].

3.1.2 Viscoelasticity of polymers

Besides efforts on developing constitutive models to address the equilibrium response (i.e. hyperelasticity) of elastomers, there also exists many models that attempt to address the observed rate dependence. To investigate the finite-strain viscoelastic properties of unfilled or filled elastomers, phenomenological viscoelastic constitutive models have been developed by Simo [71], Govindjee and Simo [72], Lion [73], Lubliner [74], Keck and Miehe [75] based on stress/strain variables. These phenomenological constitutive models are mainly used to fit existing experiment data since microscopic details about the underlying physics are not considered in the formulation of the constitutive models. Moreover, most of these reported models only capture a subset of the experimentally observed phenomena. In an attempt to overcome the disadvantage of the phenomenological models, Le Tallec et al. [76], Govindjee and Reese [77], Bergström and Boyce [78], Miehe and Göktepe [79] have developed their constitutive models for finite-strain viscoelasticity based on the tube model developed by Doi and Edwards [80]. However, these models still have several internal variables or model parameters without any physical significance, and thus have to be classified as micromechanism-inspired phenomenological models. In the information age, computationally understanding or designing materials, as suggested by materials genome initiative (MGI) [47], requires the development of fully physics-based constitutive models with all model parameters related to the molecular physical structure. The aforementioned viscoelastic constitutive models apparently do not meet this requirement.

3.2 Physics-based constitutive modeling on polymer viscoelasticity

Polymeric materials are characterized by a disparate range of spatial and temporal scales. For instance, the typical covalent bond vibrations are on the length scale of Å and time scale of sub-picoseconds. The typical size of a monomer is a nanometer with relevant dynamics in tens of picoseconds. The overall size of a single polymer chain is represented by its radius of gyration, usually between 10 and 100 nm. Depending on its surrounding environments, the relaxation of the single chain lasts about 10–100 ns, but often longer. Beyond a critical concentration, different polymer chains are coiled together with mutual uncrossability. A typical polymeric network has a size of about 1–100 nm, with a relaxation time on the order of microseconds to milliseconds. Composed of these coils and networks, the bulk polymeric materials are on the length sale of millimeters to centimeters. The relaxation and aging of these materials occur in the range of seconds, hours, days and even years. These multiple, disparate spatio-temporal scales and their interdependence among each other in terms of system behavior (i.e., bulk behavior depends on the behavior of individual polymer chains, and so forth) make it necessary to adopt a multiscale modeling technique that can correctly characterize the hierarchy of scales [49,50], if we wish to link molecular constituents with macroscopic viscoelastic properties for polymeric materials. To this end, different simulation techniques have to be used to understand these relevant physical mechanisms in the corresponding temporal and spatial scales. More importantly, a bottom-up approach should be created to systematically link these different scales together for establishing a truly multiscale modeling method for predicting the viscoelasticity of polymers.

Recently, Li and Tang [49,51] have developed a physics-based constitutive model by combining the non-affine network model [70] for hyperelasticity and a modified tube model for viscosity. All the parameters in this constitutive model carry physical significance and the model is able to capture the mechanical response of a wide range of elastomers reasonably well. Specifically, in the constitutive model, the stress response is decomposed into two parts:

$$\sigma = \sigma^E + \sigma^V \tag{1}$$

where σ^E denotes the stress stems from hyperelasticity and σ^V the stress due to viscosity. The non-affine network model yields that σ^E equals to

$$\sigma^E = \frac{1}{J}\sum_{k=1}^{3}\lambda_k\frac{\partial}{\partial\lambda_k}\left[\frac{1}{6}G_cI_1 - G_c\lambda_{max}^2\ln\left(3\lambda_{max}^2 - I_1\right) + G_e\sum_{j=1}^{3}\left(\lambda_j + \frac{1}{\lambda_j}\right)\right]v_k\otimes v_k \tag{2}$$

where $\lambda_k (k = 1, 2, 3)$ is the k_{th} principal stretch, J is the Jacobian of deformation gradient tensor F, I_1 is the first invariant of Cauchy-Green deformation tensor and v_k is the k_{th} eigenvector of Cauchy-Green deformation tensor. There are three materials parameters related to the hyperelastic stress and they all carry significant physical meanings: λ_{max} is the maximum extensibility of chains for the hyperelastic part; G_c is the cross-linking modulus of the cross-linked network; and G_e is the entanglement modulus of the cross-linked network. All these parameters can be directly related to the microstructure of cross-linked network [51], which are signatures of polymer chemistry and physics.

As we discussed before, the viscous stress originates from the diffusive behavior of free chains within the elastomer. According to the tube concept pioneered by Doi and Edwards [80], the lateral movement of the free chains is constrained within a tube-like region due to the entanglements with its neighboring chains. As a result, the chains can only move along the central line of the tube by Brownian motion.

The central line is the so-called 'primitive chain', defined as the shortest path connecting two ends of the polymer chain upon respecting uncrossability of surrounding chains. Under macroscopic loading, both the cross-linked network and free chains deform accordingly. The primitive chain deforms accordingly: the contour length of the primitive chain and the unit vector at an infinitesimal segment of the primitive chain are denoted by L_{pp0} and ν_0 respectively in the reference configuration; in the current configuration, the primitive chain deforms with contour length and the unit vector denoted as L_{pp} and ν. The mathematical formulation of σ^V is based on the configuration of the primitive chain, which is given as

$$\sigma^V = \frac{3k_BTn_v}{n_vb^2}\langle L_{pp}\rangle^2 \sum_{p=1,3,5...}^{\infty} \int_0^t \frac{8}{\pi^2\tau_d}\left[-\frac{\partial}{\partial x}E_{\alpha,1}(-x^\alpha)\right]_{x=p^2(t-t')/\tau_d} \Lambda(t,t')dt' \tag{3}$$

where k_b is the Boltzmann constant, T is the temperature. Moreover, $\langle L_{pp}\rangle$ is the expectation of primitive chain length in the current configuration and $\langle L_{pp}\rangle = \frac{\langle L_{pp0}\rangle}{4\pi}\int_{s^2}\|F\cdot\nu_0\|d^2\nu_0$, where $\int_{s^2}*d\nu_0$ represents an integration over all possible orientation of ν_0 (i.e. over a unit sphere). $E_{\alpha,1} = \sum_{k=0}^{\infty} x^k/(\alpha k)!$ is the Mittag-Leffler function. $\Lambda(t,t')$ is $\int_{s^2}\nu\otimes\nu d^2\nu\int_{s^2}\frac{1}{4\pi}\delta(\nu-\frac{F(t,t')\cdot\nu_0}{\|F(t,t')\cdot\nu_0\|})d^2\nu_0 - \frac{1}{3}I$. Here $\delta(x)$ is the Dirac delta function and I is the identity tensor. The viscous stress σ^V exhibits 6 material parameters: the number of free chains per unit volume: the polymerization degree of free chains n_v, the Kuhn length for the free chains b, the fractional order parameter for the relaxation of free chains α and the disentanglement time for the free chains τ_d, with explicit physical meanings.

In contrast to most existing finite-strain viscoelastic model for elastomers, all of the 9 material parameters in this constitutive model carry physical significance and thus each parameter can be directly obtained through molecular dynamics simulations or measured by experiments [49–51]. This enables a bottom-up approach to predict and design the macroscopic mechanical behavior of an elastomer from its molecular structure, enabling a multiscale simulation methodology to investigate the viscoelastic material behavior of elastomers [49]. The applicability of this model to predict the finite-strain viscoelastic mechanical behavior of real elastomers are demonstrated in Fig. 4b, c for un-vulcanized polymer and vulcanized polymer, respectively. Comparison between modeling results and experimental measurements indicates that the constitutive model can reasonably reproduce the experimentally observed stress-strain behaviors of vulcanized and un-vulcanized natural rubbers [49,51]. Moreover, the storage and loss moduli, viscosity, and relaxation modulus for polyisoprene and polyethylene can also be directly predicted by this constitutive model, with corresponding material law parameters determined through large scale molecular simulations [49].

To this end, because of its merits such as physics-based nature and accuracy in capturing finite-strain viscoelastic behavior, the newly developed finite-strain viscoelastic model together with the material parameters calibrated from molecular dynamics simulations can be used to model the mechanical behavior of polymer matrix in PNCs.

4 Module B: interphase toolbox

4.1 Interphase behaviors in PNCs

In PNCs, regions with altered mechanical properties are broadly called the *interphase*, and the proximity of polymer chains to solid interfaces, and thus the possibility of their interaction (either through physical or chemical interaction), is termed *confinement*. The key challenge in predicting the performance of a PNC is to quantify the spatially varying changes in interphase constitutive behavior resulting from polymer confinement and controlled by polymer-filler interaction, as a function of filler volume fraction and distribution morphology. Key insight into interphase formation and confinement effects in PNCs has come from studies on polymer thin films supported on solid substrates [81–85]. In these thin films, both the free surface at the top surface of the film and the solid supporting layer cause extremely complex changes in the behavior of the polymer.

The range and magnitude of these effects have been singled out recently by systematically varying the boundary conditions (free standing film, supported thin film, and polymer layer confined between two surfaces) and surface/polymer chemistry. Most importantly, the Schadler group [86,87], as well as the Torkelson group [82,88], have shown a quantitative equivalence between PNCs and polymer thin films with regards to glass-transition temperature (T_g) via the calculation of an equivalent metric of confinement within the nanocomposite from the distribution of filler surface-to-surface distances. Glass transition is a phenomenon inextricably linked to the constitutive (stress–strain) behavior of polymers. A non-crystallizing polymer exhibits rubbery behavior above T_g, while it behaves like a glass below T_g, with the difference between these states characterized by the dynamics and magnitude of stress relaxation. By measuring the glass transition temperature (T_g), it has been shown that the thickness of interphase in a polystyrene film is around several tens of nanometers [81]. Therefore, as the size of the fillers approaches nanoscale, the overall properties of the PNCs will depend a lot on the interphase behaviors. This finding is important because it allows for direct

prediction of the of the nanocomposite directly from thin film measurements and microstructural statistics, leveraging current capabilities in accurate computational/experimental characterization of film properties. However, it is currently unknown whether the thin-film analogy can be extended into the constitutive behavior of PNCs, most importantly the stress relaxation behavior of the polymer matrix that governs viscoelastic behavior.

Except the T_g measurements, Cheng et al. measured the mechanical properties of confined polymer films adjacent to a plane substrate through atomic force microscopy (AFM)-based indentation [83]. Two sets of polymer/substrate systems are investigated in their work: Poly(methyl methacrylate) (PMMA) on slica and alumina plates. For both systems, gradients of mechanical properties are observed in interphase regions away from the substrates. Characterized by the modulus, the thickness of the interphase region is around 100 nm, and the maximum modulus is on the material interphaes with about 50 % increase from bulk PMMA's modulus. An improved understanding of interface and interphase effects in PNCs and polymer thin films, combined with mechanistic approaches to linking polymer chemistry and confinement to relaxation metrics will pave the way for rational materials design using predictive simulations.

4.2 Molecular modeling on interphase behavior

It is well-known that the viscoelasticity of polymers origins from the chain dynamics [80,89–91]. For short, oligomer chains, their dynamics is governed by the monomeric friction, which can be described by the classical Rouse model [89]. However, when the polymerization degree N of the chain has been increased beyond the entanglement length N_e, the dynamics of chains will be hindered due to the chain connectivity and uncrossability. These topological constraints are termed as entanglements. These entanglements are commonly assumed to effectively restrict the lateral motion of individual chains into a tube-like regime, pioneered by de Gennes [90] and Doi-Edwards [80]. The so-called tube model has been developed to understand and predict the viscoelasticity of polymers, which has been considered to be the most successful theory in polymer physics in the last three decades. In the tube model, the chain moves in a one-dimensional diffusive behavior, due to the lateral confinement introduced by the entanglements. Thus, the chain can only move back and forth, or reptate, along the central axial of the tube, which is defined as the primitive path (PP). The chain can be considered to be fully relaxed when it escapes the original tube and forms another new one with neighboring chains. The critical time for the chain completely leaves its original tube is defined as the disentanglement time, τ_d. When the nanoparticles are added into the polymer network, additional constraints are introduced on the polymer chain dynamics. Consequently, the underlying entanglement network and chain relaxation can be dramatically changed by these nanoparticles, firstly observed by the authors' large scale molecular simulations [4]. Subsequently, both molecular simulations done by Grest and co-workers [92,93], and theoretical studies done by Schweizer and co-workers [94,95] have confirmed these observations. Thus, the changes of viscoelasticity of PNCs, comparing with the neat polymers, are induced by the changes of chain dynamics in PNCs [5,96]. It has been reached agreement that the polymer chain entanglements will be reduced upon adding nanoparticles [4,92,93]. However, it is still not clear how the reptation behavior of polymer chains will be affected by the added fillers. Here we *hypothesize* that the viscoelasticity of PNCs can be accurately understood by fully elucidating the polymer chain dynamics in PNCs.

To further understand the interphase behavior in PNCs, we have carried out large scale molecular dynamics (MD) simulations [6]. Due to the limitation of approachable time scale in MD simulations, only short and unentangled polymer chains are considered. Then, spherical nanoparticles with different volume fractions ϕ are infused into the polymer matrix. The dynamics of polymer matrix has been characterized by the coherent scattering function $S(q,t)$, which is defined as $S(q,t) = 1/N \sum_{i,j} \langle \exp\{i\mathbf{q}[\mathbf{r}_i(t) - \mathbf{r}_j(0)]\}\rangle$. Here $\mathbf{r}_i(t)$ and $\mathbf{r}_j(t)$ represent the positions of monomer i and j at the time t, respectively. The average $\langle * \rangle$ indicates an average over many starting states ($t = 0$) as well as orientations of the scattering vector $\mathbf{q}$. The scattering function $S(q,t)$ cannot only be quantified through the MD simulations [4,6], but also measured through neutron spin echo experiments [52,53]. Thus, $S(q,t)$ can be used to directly characterize the dynamics of chains in PNCs for interpreting their viscoelastic properties.

For neat polymers, $S(q,t)$ of short, unentangled chains can be theoretically predicted through the classical Rouse model [89], according to the monomer friction coefficient ζ. Thus, the value of ζ for neat polymer chains can be calibrated through the MD simulation results on $S(q,t)$. When the nanoparticles are added into the polymer matrix, they dynamics will be altered due to the geometric constraints applied. To understand the dynamics of chains in PNCs, we hypothesize that the $S(q,t)$ can be decomposed into two parts: one is the bulk state and the other is the interphase state, as illustrated in Fig. 5a. Then, the $S(q,t)$ can be written as $S(q,t) = A_{\text{bulk}} S_{\text{bulk}}(q,t) + A_{\text{conf}} S_{\text{conf}}(q,t)$, where A_{bulk} and A_{conf} denote the fraction of bulk and interphase states, respectively. Thus, $A_{\text{conf}} = 1 - A_{\text{bulk}}$. Here we assume that a fraction of A_{bulk} is far away from the nanoparticle surface and its dynamics is unaffected by the nanoparticle (cf. Fig. 5a). While the fraction A_{conf} is located between the bulk phase and nanoparticle with a different relaxation rate or friction coefficient ζ_{conf}, as given in Fig. 5a. By knowing

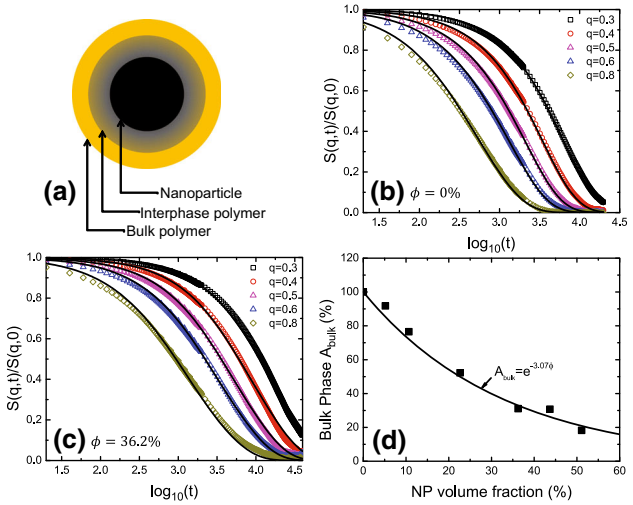

Fig. 5 Molecular simulation on interphase behavior of PNCs. **a** Proposed two layer model for interphase zone in PNC. **b** and **c** represent the dynamic structure factor results for PNCs with nanoparticle volume fractions $\phi = 0$ and 36.2%, respectively. **d** denotes the relationship between the bulk phase A_{bulk} and nanoparticle volume fraction ϕ in PNCs. The solid lines in **b** and **c** are fitted by the classical Rouse model and proposed two layer model in **a**, respectively

the monomer friction coefficient ζ from neat polymer, there are only two unknown parameters A_{conf} and ζ_{conf}, which can be fitted through the $S(q,t)$ from MD simulations. As shown in Fig. 5b, c, the $S(q,t)$ for neat polymers and PNCs with $\phi = 36.2\%$ can be well described by the Rouse model and our proposed two layer model, respectively. Moreover, by varying the volume fraction ϕ of nanoparticle, the bulk phase fraction A_{bulk} has been found to be related to ϕ as $A_{\text{bulk}} = \exp(-3.07\phi)$, shown in Fig. 5d. At the same time, the monomer friction coefficient ζ_{conf} in the interphase region is obtained, which can be related to the viscoelastic properties of interphase through the Rouse model [97]. Therefore, both the volume fraction (thickness) and mechanical properties of interphase region can be directly probed through these MD simulations.

However, the above study is limited to the short and unentangled polymer matrix. When the high entangled chains are confined by nanoparticles, their topological and dynamic properties can be dramatically altered, evidenced by the large scale molecular simulations [4,5] and experimental observations [52,53]. However, it still not clear how the reptation of chains will be affected. The viscoelasticity of neat polymers (G' and G'') scales with the loading frequency, following the combine tube relaxation, contour length fluctuation and constraint release effects [91]. These scaling behaviors have been substantially changed due to the added nanoparticles. A rigorous link between the polymer chain dynamics in PNCs and their viscoelastic behaviors will provide detailed explanations on these scaling laws.

5 Module C: microstructure toolbox

5.1 Microstructural information of PNCs

Microstructural information plays an essential role in assessing the effective properties of PNCs [7,8]. In order to capture the homogenized behaviors of a real material, a 3-dimensional structure needs to be prepared for computational multiscale modeling (e.g. FEM). The start point is always microstructure characterization through experiments; however, obtaining 3D microstructural information directly from experiments is still burdensome even with the state-of-the-art imaging techniques, especially for soft materials like PNCs [33,98]. Thus, a myriad of reconstruction techniques which computationally generate 3D microstructures based on 2D images [33,99–102] are developed to reduce the complexity and cost in the experimental stage.

Various imaging techniques can be utilized for the microstructure characterization of PNCs. The most common ones are known as SEM and transmission electron microscopy (TEM) [103], both of which are belong to 2D imaging techniques and can only observe the surface or the projection of a thin layer of a material sample. Direct 3D imaging techniques such as X-ray scattering and transmission electron microscopy tomography (TEMT) [104] are not sensitive to the microstructural conformation in the scanning direction, so that they are not capable of providing a 3D image at the RVE scale for PNCs where complex filler network are present. According to the authors' knowledge, the state-of-the-art 3D imaging technique at the RVE scale for PNCs is to serial section the 3D material and image each cross-section/layer using standard SEM or TEM. However, besides specific difficulties in serial sectioning soft materials [105], measuring in such a layer-by-layer manner is also extremely time-consuming and expensive since a high spatial resolution in the thickness direction is usually required for characterizing PNCs.

Other than characterizations purely based on experiments, a more efficient way is to computationally reconstruct 3D microstructure based on 2D images from SEM or TEM as shown in Fig. 6. By assuming the isotropicity of the 3D microstructure, a 2D image at the RVE scale would contain all the geometrical features in 3D, and theoretically no microstructural information is missing in the 2D image. In the last two decades, there has been a spectrum of reconstruction approaches, which mainly fall into three basic categories. The first category is based on N-point correlation functions, which mathematically can characterize arbitrary microstructure [99]. Various strategies are utilized to match the correlation functions of the real material sample and reconstructed ones, such as pixel/voxel moving [106], Gaussian random field-based approach [107], support vector machines [100] and generic algorithm [108]. Since correla-

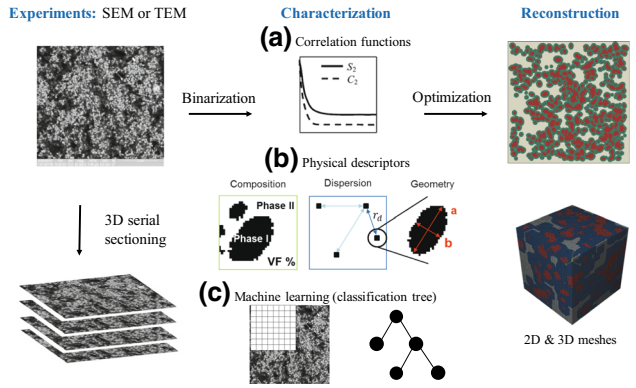

Fig. 6 Characterization and computational reconstruction of PNCs. **a** Various correlation functions are utilized to characterize the microstructure, such as two-point correlation function S_2 and two-point cluster correlation function C_2. **b** Physical descriptors are utilized to describe the microstructure. In [33], physical descriptors are classified into three categories (composition, dispersion and geometry). **c** Machine-learning methods are used to fit a model to microstructural data

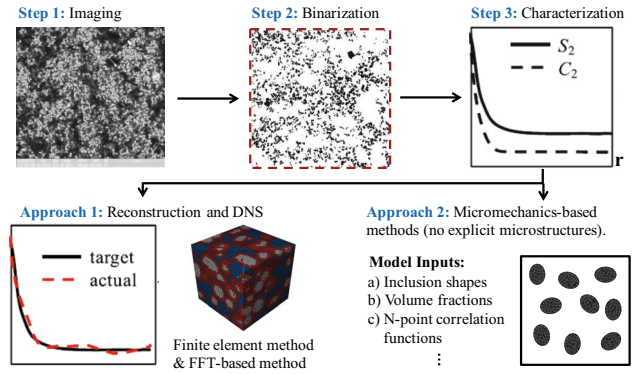

Fig. 7 Basic framework of material characterization and related homogenization of PNCs. (r : distance between a pair of points in the material; S_2 : two-point correlation; C_2 : two-point cluster correlation. 'target' refers to the desired correlation function while 'actual' refers to the one of a reconstructed RVE.) Approach 1 includes DNS methods, such as FEM and FFT-based method. Approach 2 includes various micromechanics-based methods, where the inputs are microstructural descriptors as listed

tion functions do not have clear physical meanings, a 2-point correlation function is usually not enough to capture complex microstructures and increasing the dimension of the correlation function becomes a necessary. However, evaluating and integrating higher-dimensional correlation functions are very time-consuming, making it inconvenient to use correlation functions as the design variables. The second category of reconstruction approaches is based on physical descriptors, such as filler volume fraction, the aspect ratio of fillers and nearest neighbor distance [33,101,102]. There are mainly two challenges for descriptor-based approaches: (1) finding the most important descriptors to keep the low dimensionality of microstructural characteristics; (2) predicting 3D descriptors from 2D descriptors. The last category of approaches utilizes supervised learning models and does not need predefined characteristics (e.g. correlation functions and physical descriptors). Bostanabad et al. fit a classification tree to the digitized microstructure image and efficiently reconstruct any number of statistically equivalent samples with the same learning model [109]. Although the current work based on supervised learning models is still restricted to 2D reconstruction due to a lack of good 2D-to-3D mapping algorithms, the methodology is general and shows great potential of making the reconstruction much more computationally efficient.

6 Module D: PNC homogenization toolbox

6.1 Homogenization of PNCs

Considerable effort has been put into the multiscale modeling of PNCs. Generally, the inputs of these multiscale models are (1) microstructures obtained from imaging techniques or computational reconstructions and (2) material properties of each individual constituents in the PNC. On the other hand, outputs of the models are the macroscopic material properties, such as effective storage and loss moduli. In a multiscale perspective, the developed model links microscopic information to macroscopic material behaviors, which can be further served as a homogenized constitutive relation for macroscopic simulations. Accuracy and efficiency are two critical aspects for such models; however, it is still challenging for current methods to achieve both aspects at the same time.

Direct Numerical Simulation (DNS) is the most accurate and flexible homogenization method, e.g. Finite Element Method (FEM) [110,111] and Fast Fourier Transformation (FFT)-based method [112]. For both FEM and FFT-based method, a mesh of the microstructure is needed to start the calculation as shown in Fig. 7. FFT-based methods usually require less computational resources than FEM due to its iterative manner and the high efficiency of existing FFT algorithms; However, the mesh in FFT-based method must be uniform and its convergence will be deteriorated if one material phase becomes much stiffer than the other ones. Qiao et al. [113] developed a finite element (FE) model to study the influence of the interphase percolation (overlapping) and gradients on the viscoelastic response of polymer composites. Peng et al. [114] used a FE model to analyze the effects of particle clustering and geometries of nanoparticles on the effective elastic properties of nanocomposite. Their simulations are performed at the scale of a representative-volume-element (RVE), so that the FE models are large enough to statistically represent the heterogeneous composite material. However, simulations at the RVE scale can be computationally expensive especially when the resolution of the FE mesh is high. In order to reduce the cost of each

individual simulations, Yin et al. [115] introduced a concept of statistical-volume-element (SVE), wherein the effective responses are obtained by averaging the results of several small SVEs. However, since the SVE scale is below the RVE scale, properties of realizations on the SVE scale depend on the boundary conditions and are prone to oscillation with respect to different microstructures. As a result, a large number of SVEs are usually required to narrow the variance. Such high computational cost makes DNS prohibitive for real-world multiscale engineering problems. Therefore, several approaches have been proposed to improve the efficiency of the prediction without losing substantial accuracy.

For linear viscoelastic properties of PNCs with perfectly bonded interface, the analysis in the frequency domain becomes equivalent to a linear elastic one [116], so that various micromechanics methods can be applied. As shown in Fig. 7, micromechanics methods don't need an explicit mesh of the microstructure which is a must for aforementioned DNS methods, so that burdens from computational reconstructions can be overcome. The microstructure is usually characterized by several microstructural descriptors which will be further incorporated into micromechanics models. On the other hand, since micromechanics methods usually have analytical or semi-analytical solutions based on certain assumptions in the homogenization, they are usually much more efficient than DNS methods. As the first category of micromechanics methods, Hashin and Shrikman gave the upper and lower bounds for the effective properties based on variational principles [117,118], which only depends on the volume fraction of the inclusion but ignores other key factors, such as inclusion shapes and distributions. Torquato further narrow the bounds by considering higher-order correlation functions of the microstructure [119]. The second category of the micromechanics methods methods starts with the pioneering work of Eshelby [120], which shows that the stress field is constant within an ellipsoidal inclusion embedded in an infinite matrix. Several mean-field approaches were proposed based on Eshelby's solution, such as the Mori-Tanaka method [121] and the self-consistent methods [122]. To consider arbitrary inclusion shape and strain distribution in the inclusion, Liu et al. [43] developed a self-consistent micromechanics method based on a volume integral method. As mentioned before, these theories can be generalized for use with linear viscoelasticity of polymer composite by performing the Fourier transformation of the constitutive law. Liu et al. [123] used the Mori-Tanaka method to evaluate the reinforcing efficiency of inclusions on the storage and loss moduli in polymer nanocomposite. Diani et al. [124] used the 3-phase and 4-phase self-consistent methods to investigate the role of interphase in the carbon-black filled styrene butadiene rubbers.

Recently, Liu et al. proposed a mechanistic and data-driven approach called "self-consistent clustering analysis"

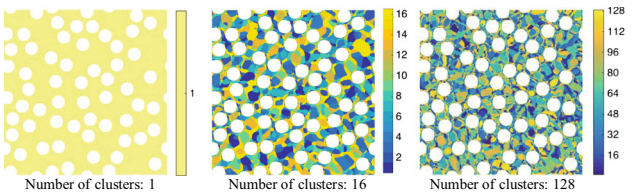

Fig. 8 Clustering results in the matrix of a 2D composite with 1, 16 and 128 clusters. The mesh size of the original DNS is 600 × 600, and a set of DNS under 3 orthogonal loading conditions (or 6 in 3D) is needed for constructing the database in the offline stage [54]

(SCA) for homogenizing elastic, viscoelastic and plastic heterogeneous materials [54,125]. By incorporating data compression algorithms (e.g. k-means clustering) in the offline (or training) stage, material points with similar mechanical behaviors are grouped into clusters, so that the number of degree-of-freedoms (DOF) in the online (or predicting) stage can be greatly reduced. Clustering results based upon the elastic strain concentration tensor in a 2D composite are provided in Fig. 8, and this data compression approach can be applied to both 2D and 3D heterogeneous materials with arbitrary microstructures, such as clusters of nanoparticles and interacting interphases in PNCs. In the online stage, the homogenization of each material cluster is achieved by solving the Lippmann-Schwinger equation self-consistently. For elastic properties, using the same database built on a certain selection of phase properties in the offline stage, SCA predicts the effective properties of new materials with different selections of phase properties accurately with only a small number of clusters, so it is much more efficient than a full-field DNS. Moreover, it also shows great potential of modeling inelastic material behaviors in PNCs, such as the Payne effect.

7 Perspective and future works

Computational methods that could facilitate accurate predictions of PNCs can speed up materials design processes aimed at achieving particular viscoelastic properties. PNCs are ubiquitously used in engineering materials ranging from tire to structural materials used in the built environment and aerospace structures. By improving dynamic mechanical performance of these materials, it will be possible to create materials with highly-tunable, predictable relaxation properties. Advances in materials discovery using computation has now become a national priority because it is now known that the slow nature of the materials development process will become the central bottleneck in the way of technological innovation in the near future. In additional to these anticipated societal benefits, fundamental research on PNCs provides unique opportunities to generate impact

by integrating new physical concepts into the mechanics of composites. In conclusion, understanding and designing PNCs with unprecedented mechanical properties via multiscale simulation is an emerging and exciting research field. Among a variety list of potentially intriguing directions for future research, several areas present particularly pressing needs.

(i) Physically understanding on the material behaviors of the interface between nanoparticle and polymer matrix in PNCs is one of the holy grail in polymer science. It is critical to develop new experimental techniques to characterize and quantitatively measure the mechanical and topological properties of the interphase region, such as the variation of polymer chain dynamics and interphase thickness, which are not accessible by existing experimental tools. Moreover, the computational methods, such as molecular dynamics, can be applied to understand the structure and dynamic properties of chains in vicinity of nanoparticles, as shown in Sect. 3.2. However, further studies on high entangled chains are still beyond the capability of current methods, as the relaxation time of the chain $\tau_d \sim N^3$, where N is the polymerization degree. Therefore, the corresponding simulations need multiple years to finish, given by the current state-of-the art supercomputers. Development of more advanced computational method could benefit the fundamental understandings on the interfacial properties in PNCs through large scale computation.

(ii) The development of new physics-based viscoelastic models for PNCs with all model parameters connected to molecular structures is highly desired. In this work, we have introduced an newly developed physics-based viscoelastic constitutive model for polymer matrix. However, the key challenges and opportunities reside in the fact that the model cannot capture the influence of nanofiller on the mechanical response of PNCs. To this end, descriptors such as volume fraction and size of nanofillers may need to be included in a physical-based viscoelastic model for modeling PNCs. Distinct from existing constitutive models for filled polymer, the new model will have all model parameters carrying physical significance and thus enable bottom-up material design of PNCs.

(iii) Advanced homogenization techniques of PNCs are desired, especially for nonlinear properties such as hyperelasticity. Existing DNS methods are accurate and flexible, but may be prohibited from design purpose due to the extremely high computational cost. On the other hand, most analytical micromechanics methods are limited to certain microstructure (e.g. spherical inclusions embedded in the matrix) and small strain assumption. A promising way is to enhance the homogenization with database precomputed by DNS methods as what has been done in SCA [54]. The challenging parts of data-driven approaches are always how to construct the database and how to extract data from the database efficiently.

(iv) It is necessary to study the mechanical behavior of emerging PNCs and their derivatives such as graphene-filled PNCs and nanocomposite hydrogels. Owing to their unprecedented mechanical, thermal and electrical properties, these new PNCs have wide applications such as sensors [126], electrodes, stimuli responsive devices [127], tissue scaffolds [128] and drug delivery agents [129]. Because of the new structural and physical characteristics of these PNCs (e.g. the high content of water in nanocomposite hydrogels), understanding the mechanical behavior of these new PNCs necessitates development of synergistically integrated modeling and high-fidelity experiments.

Finally, we note that tackling the above problems presents many challenges and opportunities for mechanicians and experimentalists. Hopefully, the synergistically integrated multiscale experiment and modeling will shed light on the understanding, design, and optimization of new PNCs by linking molecular level parameters to macroscopic material properties/performance.

Acknowledgements This project was funded by the Deanship of Scientific Research (DSR), King Abdulaziz University, under Grant No.(7-135-1434 HiCi). This research was supported in part through the computational resources and staff contributions provided for the Booth Engineering Center for Advanced Technology (BECAT) at University of Connecticut.

References

1. Vilgis TA, Heinrich G, Klüppel M (2009) Reinforcement of polymer nano-composites: theory, experiments and applications. Cambridge University Press, Cambridge
2. Ramanathan T, Abdala AA, Stankovich S, Dikin DA, Herrera-Alonso M, Piner RD, Adamson DH, Schniepp HC, Chen X, Ruoff RS et al (2008) Functionalized graphene sheets for polymer nanocomposites. Nat Nanotechnol 3(6):327–331
3. Ramanathan T, Liu H, Brinson LC (2005) Functionalized swnt/polymer nanocomposites for dramatic property improvement. J Polym Sci B 43(17):2269–2279
4. Li Y, Kröger M, Liu WK (2012) Nanoparticle effect on the dynamics of polymer chains and their entanglement network. Phys Rev Lett 109(11):118001
5. Li Y, Kröger M, Liu WK (2012) Nanoparticle geometrical effect on structure, dynamics and anisotropic viscosity of polyethylene nanocomposites. Macromolecules 45(4):2099–2112
6. Li Y, Kröger M, Liu WK (2014) Dynamic structure of unentangled polymer chains in the vicinity of non-attractive nanoparticles. Soft Matter 10(11):1723–1737
7. Moore JA, Li Y, O'Connor DT, Stroberg W, Liu Wing Kam (2015) Advancements in multiresolution analysis. Int J Numer Methods Eng 102(3–4):784–807
8. Greene MS, Li Y, Chen W, Liu WK (2014) The archetype-genome exemplar in molecular dynamics and continuum mechanics. Comp Mech 53(4):687–737

9. Wang MJ (1998) Effect of polymer-filler and filler-filler interactions on dynamic properties of filled vulcanizates. Rubber Chem Technol 71(3):520–589
10. Kahn Ribeiro S, Kobayashi S, Beuthe M, Gasca J, Greene D, Lee DS, Muromachi Y, Newton PJ, Plotkin S, Sperling D, Wit R, Zhou PJ (2007) Transport and its infrastructure. In: Metz B, Davidson OR, Bosch PR, Dave R, Meyer LA (eds) Climate change 2007: mitigation. Contribution of working group III to the fourth assessment report of the intergovernmental panel on climate change. Cambridge University Press, Cambridge, New York
11. Pearce JM, Hanlon JT (2007) Energy conservation from systematic tire pressure regulation. Energy Policy 35(4):2673–2677
12. Einstein A (1956) Investigations on the theory of the Brownian movement. Courier Corporation. Dover Publications Inc., New York
13. Smallwood HM (1944) Limiting law of the reinforcement of rubber. J Appl Phys 15(11):758–766
14. Ahmed SaFRJ, Jones FR (1990) A review of particulate reinforcement theories for polymer composites. J Mater Sci 25(12):4933–4942
15. Shao-Yun F, Feng XQ, Lauke B, Mai YW (2008) Effects of particle size, particle/matrix interface adhesion and particle loading on mechanical properties of particulate-polymer composites. Compos B 39(6):933–961
16. Bigg DM (1987) Mechanical properties of particulate filled polymers. Polymer Composites 8(2):115–122
17. Li S, Sauer RA, Wang G (2007) The eshelby tensors in a finite spherical domain part i: theoretical formulations. J Appl Mech 74(4):770–783
18. Li S, Wang G, Sauer RA (2007) The eshelby tensors in a finite spherical domain part ii: applications to homogenization. J Appl Mech 74(4):784–797
19. Shi C, Qingsong T, Fan H, Rios CAO, Li S (2016) Interphase models for nanoparticle-polymer composites. J Nanomech Micromech 6(2):04016003
20. Dickie RA (1973) Heterogeneous polymer-polymer composites. i. theory of viscoelastic properties and equivalent mechanical models. J Appl Polym Sci 17(1):45–63
21. Finegan IC, Gibson RF (1999) Recent research on enhancement of damping in polymer composites. Compos Struct 44(2):89–98
22. Li K, Gao X-L, Roy AK (2006) Micromechanical modeling of viscoelastic properties of carbon nanotube-reinforced polymer composites. Mech Adv Mater Struct 13(4):317–328
23. Fisher FT, Brinson LC (2001) Viscoelastic interphases in polymer-matrix composites: theoretical models and finite-element analysis. Compos Sci Technol 61(5):731–748
24. Bergström JS, Boyce MC (2001) Constitutive modeling of the time-dependent and cyclic loading of elastomers and application to soft biological tissues. Mech Mater 33(9):523–530
25. Bergström JS, Boyce MC (2000) Large strain time-dependent behavior of filled elastomers. Mech Mater 32(11):627–644
26. Bergstrom JS, Boyce MC (1999) Mechanical behavior of particle filled elastomers. Rubb Chem Technol 72(4):633–656
27. O'Keeffe SC, Tang S, Kopacz AM, Smith J, Rowenhorst DJ, Spanos G, Liu WK, Olson GB (2015) Multiscale ductile fracture integrating tomographic characterization and 3-d simulation. Acta Mater 82:503–510
28. Tang S, Kopacz AM, Chan S, Olson GB, Liu WK et al (2013) Three-dimensional ductile fracture analysis with a hybrid multiresolution approach and microtomography. J Mech Phys Solids 61(11):2108–2124
29. Tang S, Kopacz AM, O'Keeffe SC, Olson GB, Liu WK (2013) Concurrent multiresolution finite element: formulation and algorithmic aspects. Comput Mech 52(6):1265–1279
30. Hua Deng Y, Liu DG, Dikin DA, Putz KW, Wei Chen L, Brinson C, Burkhart C, Poldneff M, Jiang B et al (2012) Utilizing real and statistically reconstructed microstructures for the viscoelastic modeling of polymer nanocomposites. Compos Sci Technol 72(14):1725–1732
31. Breneman CM, Brinson LC, Schadler LS, Natarajan B, Krein M, Wu K, Morkowchuk L, Li Y, Deng H, Xu H (2013) Stalking the materials genome: A data-driven approach to the virtual design of nanostructured polymers. Adv Funct Mater 23(46):5746–5752
32. Liu Y, Greene MS, Chen W, Dikin DA, Liu WK (2013) Computational microstructure characterization and reconstruction for stochastic multiscale material design. Comp Aided Des 45(1):65–76
33. Hongyi X, Li Y, Brinson C, Chen W (2014) A descriptor-based design methodology for developing heterogeneous microstructural materials system. J Mech Des 136(5):051007
34. Hongyi X, Liu R, Choudhary A, Chen W (2015) A machine learning-based design representation method for designing heterogeneous microstructures. J Mech Des 137(5):051403
35. Papon A, Saalwächter K, Schaler K, Guy L, Lequeux F, Montes H (2011) Low-field nmr investigations of nanocomposites: polymer dynamics and network effects. Macromolecules 44(4):913–922
36. Papon A, Montes H, Hanafi M, Lequeux F, Guy L, Saalwächter K (2012) Glass-transition temperature gradient in nanocomposites: evidence from nuclear magnetic resonance and differential scanning calorimetry. Phys Rev Lett 108(6):065702
37. Starr FW, Schrøder TB, Glotzer SC (2001) Effects of a nanoscopic filler on the structure and dynamics of a simulated polymer melt and the relationship to ultrathin films. Phys Rev E 64(2):021802
38. Starr FW, Schrøder TB, Glotzer SC (2002) Molecular dynamics simulation of a polymer melt with a nanoscopic particle. Macromolecules 35(11):4481–4492
39. Margarita Krutyeva A, Wischnewski MM, Willner L, Maiz J, Mijangos Carmen, Arantxa Arbe J, Colmenero AR, Holderer O et al (2013) Effect of nanoconfinement on polymer dynamics: surface layers and interphases. Phys Rev Lett 110(10):108303
40. Glomann T, Schneider GJ, Allgaier J, Radulescu A, Lohstroh W, Farago B, Richter D (2013) Microscopic dynamics of polyethylene glycol chains interacting with silica nanoparticles. Phys Rev Lett 110(17):178001
41. Wood CD, Ajdari A, Burkhart CW, Putz KW, Brinson LC (2016) Understanding competing mechanisms for glass transition changes in filled elastomers. Compos Sci Technol 127:88–94
42. Liu H, Brinson LC (2006) A hybrid numerical-analytical method for modeling the viscoelastic properties of polymer nanocomposites. J Appl Mech 73(5):758–768
43. Liu Z, Moore JA, Aldousari SM, Hedia HS, Asiri SA, Liu WK (2015) A statistical descriptor based volume-integral micromechanics model of heterogeneous material with arbitrary inclusion shape. Comput Mech 55(5):963–981
44. Moore JA, Ma R, Domel AG, Liu WK (2014) An efficient multiscale model of damping properties for filled elastomers with complex microstructures. Compos B 62:262–270
45. Song Y, Zheng Q (2011) Application of two phase model to linear dynamic rheology of filled polymer melts. Polymer 52(26):6173–6179
46. Simmons DS (2016) An emerging unified view of dynamic interphases in polymers. Macromol Chem Phys 217(2):137–148
47. Materials genome initiative. https://www.whitehouse.gov/mgi. Accessed 2 Mar 2016
48. Li Y, Kröger M, Liu WK (2011) Primitive chain network study on uncrosslinked and crosslinked cis-polyisoprene polymers. Polymer 52(25):5867–5878
49. Li Y, Tang S, Abberton BC, Kröger M, Burkhart C, Jiang B, Papakonstantopoulos GJ, Poldneff M, Liu WK (2012) A

predictive multiscale computational framework for viscoelastic properties of linear polymers. Polymer 53(25):5935–5952
50. Li Y, Abberton BC, Kröger M, Liu WK (2013) Challenges in multiscale modeling of polymer dynamics. Polymers 5(2):751–832
51. Li Y, Tang S, Kröger M, Liu WK (2016) Molecular simulation guided constitutive modeling on finite strain viscoelasticity of elastomers. J Mech Phys Solids 88:204–226
52. Schneider GJ, Nusser K, Willner L, Falus P, Richter D (2011) Dynamics of entangled chains in polymer nanocomposites. Macromolecules 44(15):5857–5860
53. Schneider GJ, Nusser K, Neueder S, Brodeck M, Willner L, Farago B, Holderer O, Briels WJ, Richter D (2013) Anomalous chain diffusion in unentangled model polymer nanocomposites. Soft Matter 9(16):4336–4348
54. Liu Z, Bessa MA, Liu WK (2016) Self-consistent clustering analysis. Comp Methods Appl Mech Eng 306:319–341
55. Hausler K, Sayir MB (1995) Nonlinear viscoelastic response of carbon black reinforced rubber derived from moderately large deformations in torsion. J Mech Phys Solids 43(2):295–318
56. Ferry JD (1980) Viscoelastic properties of polymers. Wiley, New York
57. Tang S, Greene MS, Liu WK (2012) Two-scale mechanism-based theory of nonlinear viscoelasticity. J Mech Phys Solids 60(2):199–226
58. Mooney M (1940) A theory of large elastic deformation. J Appl Phys 11(9):582–592
59. Rivlin RS (1948) Large elastic deformations of isotropic materials. iv. further developments of the general theory. Philos Trans R Soc Lond A 241(835):379–397
60. Ogden RW (1972) Large deformation isotropic elasticity-on the correlation of theory and experiment for incompressible rubberlike solids. Proc R Soc Lond A 326:565–584
61. Yeoh OH (1993) Some forms of the strain energy function for rubber. Rubber Chem Technol 66(5):754–771
62. Gent AN (1996) A new constitutive relation for rubber. Rubb Chem Technol 69(1):59–61
63. Marckmann G, Verron E (2006) Comparison of hyperelastic models for rubber-like materials. Rubb Chem Technol 79(5):835–858
64. Treloar LRG (1943) The elasticity of a network of long-chain moleculesii. Trans Faraday Soc 39:241–246
65. Kuhn W, Grün F (1942) Beziehungen zwischen elastischen konstanten und dehnungsdoppelbrechung hochelastischer stoffe. Kolloid-Zeitschrift 101(3):248–271
66. Arruda EM, Boyce MC (1993) A three-dimensional constitutive model for the large stretch behavior of rubber elastic materials. J Mech Phys Solids 41(2):389–412
67. Edwards SF, Vilgis Th (1986) The effect of entanglements in rubber elasticity. Polymer 27(4):483–492
68. Kaliske M, Heinrich G (1999) An extended tube-model for rubber elasticity: statistical-mechanical theory and finite element implementation. Rubb ChemTechnol 72(4):602–632
69. Miehe C, Göktepe S, Lulei F (2004) A micro-macro approach to rubber-like materials part i: the non-affine micro-sphere model of rubber elasticity. J Mech Phys Solids 52(11):2617–2660
70. Davidson JD, Goulbourne NC (2013) A nonaffine network model for elastomers undergoing finite deformations. J Mech Phys Solids 61(8):1784–1797
71. Simo JC (1987) On a fully three-dimensional finite-strain viscoelastic damage model: formulation and computational aspects. Comp Methods Appl Mech Eng 60(2):153–173
72. Govindjee S, Simo JC (1992) Mullins effect and the strain amplitude dependence of the storage modulus. Int J Solids Struct 29(14):1737–1751
73. Lion A (1996) A constitutive model for carbon black filled rubber: experimental investigations and mathematical representation. Continuum Mech Thermodyn 8(3):153–169
74. Lubliner J (1985) A model of rubber viscoelasticity. Mech Res Commun 12(2):93–99
75. Keck J, Miehe C (1997) An eulerian overstress-type viscoplastic constitutive model in spectral form formulation and numerical implementation. Comput Plast 1:997–1003
76. Le Tallec P, Rahier C, Kaiss A (1993) Three-dimensional incompressible viscoelasticity in large strains: formulation and numerical approximation. Comp Methods Appl Mech Eng 109(3–4):233–258
77. Govindjee S, Reese S (1997) A presentation and comparison of two large deformation viscoelasticity models. J Eng Mater Technol 119(3):251–255
78. Bergström JS, Boyce MC (1998) Constitutive modeling of the large strain time-dependent behavior of elastomers. J Mech Phys Solids 46(5):931–954
79. Miehe C, Göktepe S (2005) A micro-macro approach to rubber-like materials. part ii: the micro-sphere model of finite rubber viscoelasticity. J Mech Phys Solids 53(10):2231–2258
80. Doi M, Edwards SF (1986) The theory of polymer dynamics, international series of monographs on physics. Clarendon Press, Oxford
81. Ellison CJ, Torkelson JM (2003) The distribution of glass-transition temperatures in nanoscopically confined glass formers. Nat Mater 2(10):695–700
82. Rittigstein P, Priestley RD, Broadbelt LJ, Torkelson JM (2007) Model polymer nanocomposites provide an understanding of confinement effects in real nanocomposites. Nat Mater 6(4):278–282
83. Cheng X, Putz KW, Wood CD, Brinson LC (2014) Characterization of local elastic modulus in confined polymer films via afm indentation. Macromol Rapid Commun 36:391–397
84. Cheng X, Putz KW, Wood CD, Brinson LC (2015) Characterization of local elastic modulus in confined polymer films via afm indentation. Macromol Rapid Commun 36(4):391–397
85. Watcharotone S, Wood CD, Friedrich R, Chen X, Qiao Rui, Putz Karl, Brinson L Catherine (2011) Interfacial and substrate effects on local elastic properties of polymers using coupled experiments and modeling of nanoindentation. Adv Eng Mater 13(5):400–404
86. Natarajan B, Li Y, Deng H, Brinson LC, Schadler Linda S (2013) Effect of interfacial energetics on dispersion and glass transition temperature in polymer nanocomposites. Macromolecules 46(7):2833–2841
87. Ash BJ, Siegel RW, Schadler LS (2004) Glass-transition temperature behavior of alumina/pmma nanocomposites. J Polym Sci B 42(23):4371–4383
88. Roth CB, McNerny KL, Jager WF, Torkelson JM (2007) Eliminating the enhanced mobility at the free surface of polystyrene: fluorescence studies of the glass transition temperature in thin bilayer films of immiscible polymers. Macromolecules 40(7):2568–2574
89. Rouse PE Jr (1953) A theory of the linear viscoelastic properties of dilute solutions of coiling polymers. J Chem Phys 21(7):1272–1280
90. De Gennes P-G (1979) Scaling concepts polymer physics. Cornell University Press, New York
91. McLeish TCB (2002) Tube theory of entangled polymer dynamics. Adv Phys 51(6):1379–1527
92. Kalathi JT, Grest GS, Kumar SK (2012) Universal viscosity behavior of polymer nanocomposites. Phys Rev Lett 109(19):198301
93. Kalathi JT, Kumar SK, Rubinstein M, Grest GS (2015) Rouse mode analysis of chain relaxation in polymer nanocomposites. Soft Matter 11(20):4123–4132

94. Yamamoto U, Schweizer KS (2013) Theory of entanglements and tube confinement in rod-sphere nanocomposites. ACS Macro Lett 2(11):955–959
95. Yamamoto U, Schweizer KS (2013) Spatially dependent relative diffusion of nanoparticles in polymer melts. J Chem Phys 139(6):064907
96. Nusser K, Schneider GJ, Richter D (2013) Rheology and anomalous flow properties of poly (ethylene-alt-propylene)-silica nanocomposites. Macromolecules 46(15):6263–6272
97. Abberton BC, Liu WK, Keten S (2015) Anisotropy of shear relaxation in confined thin films of unentangled polymer melts. Macromolecules 48(20):7631–7639
98. Yeong CLY, Torquato S (1998) Reconstructing random media. ii. three-dimensional media from two-dimensional cuts. Phys Rev E 58(1):224
99. Torquato S (2013) Random heterogeneous materials: microstructure and macroscopic properties, vol 16. Springer, Berlin
100. Sundararaghavan V, Zabaras N (2005) Classification and reconstruction of three-dimensional microstructures using support vector machines. Comput Mater Sci 32(2):223–239
101. Jean A, Jeulin D, Forest S, Cantournet S, Nguyen Franck (2011) A multiscale microstructure model of carbon black distribution in rubber. J Microsc 241(3):243–260
102. Laiarinandrasana L, Jean A, Jeulin D, Forest S (2012) Modelling the effects of various contents of fillers on the relaxation rate of elastomers. Mater Des 33:75–82
103. Karasek L, Sumita M (1996) Characterization of dispersion state of filler and polymer-filler interactions in rubber-carbon black composites. J Mater Sci 31(2):281–289
104. Chen L, Zhou W, Jie L, Li J, Zhang W, Huang N, Lihui W, Li L (2015) Unveiling reinforcement and toughening mechanism of filler network in natural rubber with synchrotron radiation x-ray nano-computed tomography. Macromolecules 48(21):7923–7928
105. Egerton RF, Li P, Malac M (2004) Radiation damage in the tem and sem. Micron 35(6):399–409
106. Saheli G, Garmestani H, Adams BL (2004) Microstructure design of a two phase composite using two-point correlation functions. J Comp Aided Mater Des 11(2–3):103–115
107. Roberts AP (1997) Statistical reconstruction of three-dimensional porous media from two-dimensional images. Phys Rev E 56(3):3203
108. Basanta D, Miodownik MA, Holm EA, Bentley PJ (2005) Using genetic algorithms to evolve three-dimensional microstructures from two-dimensional micrographs. Metallurgical Mater Trans A 36(7):1643–1652
109. Bostanabad R, Bui AT, Xie W, Apley DW, Chen W (2016) Stochastic microstructure characterization and reconstruction via supervised learning. Acta Mater 103:89–102
110. Feyel F, Chaboche JL (2000) Fe 2 multiscale approach for modelling the elastoviscoplastic behaviour of long fibre sic/ti composite materials. Comp Methods Appl Mech Eng 183(3):309–330
111. Belytschko T, Liu WK, Moran B, Elkhodary K (2013) Nonlinear finite elements for continua and structures. Wiley, New York
112. Moulinec H, Suquet P (1998) A numerical method for computing the overall response of nonlinear composites with complex microstructure. Comp Methods Appl Mech Eng 157(12):69–94
113. Qiao R, Brinson LC (2009) Simulation of interphase percolation and gradients in polymer nanocomposites. Compos Sci Technol 69(3):491–499
114. Peng RD, Zhou HW, Wang HW, Mishnaevsky L (2012) Modeling of nano-reinforced polymer composites. Comput Mater Sci 60:19–31
115. Yin X, Chen W, To A, McVeigh C, Liu WK (2008) Statistical volume element method for predicting microstructure-constitutive property relations. Comp Methods Appl Mech Eng 197(43):3516–3529
116. Brinson HF, Brinson LC (2007) Polymer engineering science and viscoelasticity: an introduction. Springer, New York
117. Hashin Z (1962) The elastic moduli of heterogeneous materials. J Appl Mech 29(1):143–150
118. Hashin Z, Shtrikman S (1963) A variational approach to the theory of the elastic behaviour of multiphase materials. J Mech Phys Solids 11(2):127–140
119. Torquato S (1991) Random heterogeneous media: microstructure and improved bounds on effective properties. Appl Mech Rev 44(2):37–76
120. Eshelby JD (1957) The determination of the elastic field of an ellipsoidal inclusion, and related problems. Proc R Soc Lond A 241:376–396
121. Mori T, Tanaka K (1973) Average stress in matrix and average elastic energy of materials with misfitting inclusions. Acta Metallurgica 21(5):571–574
122. Hill R (1965) A self-consistent mechanics of composite materials. J Mech Phys Solids 13(4):213–222
123. Liu H, Brinson L Catherine (2008) Reinforcing efficiency of nanoparticles: a simple comparison for polymer nanocomposites. Compos Sci Technol 68(6):1502–1512
124. Diani J, Gilormini P, Merckel Y, Vion-Loisel F (2013) Micromechanical modeling of the linear viscoelasticity of carbon-black filled styrene butadiene rubbers: The role of the filler-rubber interphase. Mech Mater 59:65–72
125. Liu Z, Moore JA, Liu WK (2016) An extended micromechanics method for probing interphase properties in polymer nanocomposites. J Mech Phys Solids 95:663–680
126. Chen L, Chen GH, Lu L (2007) Piezoresistive behavior study on finger-sensing silicone rubber/graphite nanosheet nanocomposites. Adv Func Mater 17(6):898–904
127. Xiao X, Xie T, Cheng YT (2010) Self-healable graphene polymer composites. J Mater Chem 20(17):3508–3514
128. Yang S, Wang J, Tan H, Zeng F, Liu C (2012) Mechanically robust pegda-msns-oh nanocomposite hydrogel with hierarchical meso-macroporous structure for tissue engineering. Soft Matter 8(34):8981–8989
129. Moghadam MN, Kolesov V, Vogel A, Klok HA, Pioletti DP (2014) Controlled release from a mechanically-stimulated thermosensitive self-heating composite hydrogel. Biomaterials 35(1):450–455